



# A new real-time multi-agent system for under frequency load shedding in a smart grid context

Athila Quaresma Santos<sup>a</sup>, Renato Machado Monaro<sup>b,\*</sup>, Denis Vinicius Coury<sup>c</sup>, Mario Oleskovicz<sup>c</sup>

<sup>a</sup> Center for Energy Informatics, Mærsk Mc-Kinney Møller Institut, University of Southern Denmark, Odense, Denmark

<sup>b</sup> Department of Electric Energy and Automation Engineering, Polytechnic School, University of São Paulo, São Paulo, SP, Brazil

<sup>c</sup> Department of Electrical and Computer Engineering, São Carlos School of Engineering, University of São Paulo, São Carlos, SP, Brazil

## ARTICLE INFO

MSC:  
00-01  
99-00

### Keywords:

Automatic under frequency load shedding  
Multi-agent system  
Real time closed loop  
Smart grids  
Electric power system analysis

## ABSTRACT

Automatic under frequency load shedding schemes need to be carefully designed in order to reduce the risk of widespread system collapse. This paper proposes a centralized hierarchical multi-agent system that coordinates various stages of monitoring and decision making processes. The main contribution is to improve traditional contingency response algorithms such as load shedding schemes, taking advantage of the future smart grid infrastructure. The multi-agent system seeks for a minimum amount of load disconnection in a short period of time, causing the least possible disturbance in the system frequency. A hardware-in-the-loop simulation of a full electric power system using a real time digital simulator was utilized. The solution was embedded in a real time system, consisting of hardware and software, to test and validate the proposed methodology. In addition, the studied methodology was compared with two other load shedding philosophies through a load shedding metric score. Shedding was carried out in a single step and the amount of disconnected load was close to the dynamic power unbalance. The results show that it is possible to improve the traditional load shedding philosophy schemes and use advanced communication infrastructure, monitoring and embedded processing capabilities to provide better stability and reduce unnecessary load disconnections from the system.

## 1. Introduction

It is well known that electric energy consumption has grown worldwide. Its increasing demand generally leads the current infrastructure to overload conditions. This growth is accompanied by the need for more robust and reliable Electric Power System (EPSs), as well as modern techniques to operate and protect them. The large number of blackouts worldwide in recent years also reinforces this unfavorable scenario [1,2].

Among the unwelcome EPS failures, one of the most critical ones that causes sequential tripping leading to blackouts is the under frequency condition. This situation is a result of an unbalance between active power supply and demand. Therefore, keeping frequency stability has been one of the main challenges faced by electrical engineers. Considering this, the Automatic Under Frequency Load Shedding (AUFLS) process was proposed with the objective of restoring the supply/demand by reducing the system load, avoiding the general collapse of the system [3]. Moreover, poorly designed (AUFLS) may result in insufficient or excessive load shedding schemes.

Since the conception of the instantaneous frequency method

proposed by [4], several improvements have been proposed in order to obtain better results in the control of overloaded systems. One of the most recognised algorithms is the Rate Of Change Of Frequency (ROCOF) which proposes an adaptive method based on the initial slope of the rate of change of frequency [5,6]. However, modern methods that use computerized management and analyze network topology and process optimization are necessary [7]. A growing number of load shedding techniques have been reported in recent years using alternative approaches, such as intelligent tools [8,9], remote monitoring solutions and the use of Multi-Agent System (MAS) [10,11], among others. They have become attractive alternatives to compensate failures of traditional models, mainly to develop optimized algorithms that provide good results against the static approach [12,13].

The existing methods present certain limitations that under specific operating conditions may have an impact on the correct operation of the (AUFLS) project. Usually, shedding schemes use several time steps to adequate the frequency level. This is detrimental for the entire system that can experience longer instability times and unnecessary delays that can cause the trip of other protection systems. Depending on how the loads are distributed among the feeders and their respective

\* Corresponding author.

E-mail address: [monaro@usp.br](mailto:monaro@usp.br) (R.M. Monaro).

<https://doi.org/10.1016/j.epsr.2019.04.029>

Received 31 October 2018; Received in revised form 25 April 2019; Accepted 25 April 2019

Available online 16 May 2019

0378-7796/ © 2019 Elsevier B.V. All rights reserved.

priorities, unnecessary removal of large blocks can cause excessive overshoot of frequency levels. Moreover, it is common to use more than one shedding philosophy, such as instantaneous frequency and (ROCOF) methods, because the latter is more susceptible to noise values and discontinuous changes caused by the frequency calculation algorithm.

Most of the studies use theoretical analysis and do not consider the issues when employing real-time applications [14] and the execution of algorithms in embedded hardware systems, such as Phasor Measurement Unit (PMUs) for measuring real-time voltage and current phasor data, as well as the frequency of critical monitored points of the system [15–17]. They also poorly apply the capabilities provided by the future Smart Grid (SGs), such as improved telecommunication techniques, advanced communication protocols, such as the IEC 61850, applied to power systems and two-way communication systems for connected and pervasive environments and the exploration of Wide Area Measurement System (WAMSs) for monitoring larger areas of the EPS [18–20]. This kind of infrastructure also allows pervasive computing capabilities as attractive alternatives concerning modernisation, providing improvements in control, management, efficiency, protection and reliability of the system [7,21,22]. Considering this, one can take advantage of these resources in order to improve existing (AUFLS) algorithms.

The purpose of this study is to develop a new (AUFLS) scheme using a MAS with a centralized hierarchical architecture. In order to do this, an MAS was embedded in a real-time integrated platform, consisting of hardware and software. The Hardware-In-the-Loop (HIL) configuration was made possible using the IEC 61850 communication protocol to exchange *Generic Object Oriented Substation Events* (GOOSE) type messages between power substations devices. The EPS was simulated using data obtained from a Real Time Digital Simulator (RTDS). The MAS aims to disconnect a minimum amount of loads in the shortest period of time with the least disturbance of the system's frequency.

The main contribution of this paper is to improve traditional contingency response algorithms, taking advantage of the current SG infrastructure, such as for load shedding schemes that were designed several decades ago with huge technological restraints and are still being used in EPSs of today. The proposed scheme established new parameters for time response, frequency accommodation time and frequency stability, considering both underfrequency and overfrequency rebound caused by the disconnection of large load blocks. It also indicates in only one step a good approximation for the amount of load that needs to be shed.

In order to compare the performance of the proposed method, a load shedding scoring evaluation metric was used. This scoring metric was proposed by the authors in [23] to evaluate the performance of individual load shedding schemes that do not depend on the characteristics of a specific EPS or the load shedding philosophy used. The results of the proposed methodology were compared with two other load shedding philosophies widely used in (AUFLS) schemes [24]: the instantaneous frequency of the system ( $f$ ) and the Rate Of Change Of Frequency (ROCOF) ( $\frac{df}{dt}$ ). The results showed that the proposed approach improves the management, control and decision making of load shedding processes, ensuring the system's stability and a minimal load discontinuity when compared with the other two philosophies.

## 2. The multi-agent system solution

The MAS approach proposed in this paper is based on a multi-hierarchical centralized control structure, as illustrated in Fig. 1. There are three hierarchical layers. As can be seen, system measurements, system's topology and the decision-making process are independent layers and can exchange information. The proposed method does not model each bus as an agent. Besides, if the monitored buses are on the same substation, the agents can be allocated to the same processing unit, as the data will be transmitted using a network infrastructure.

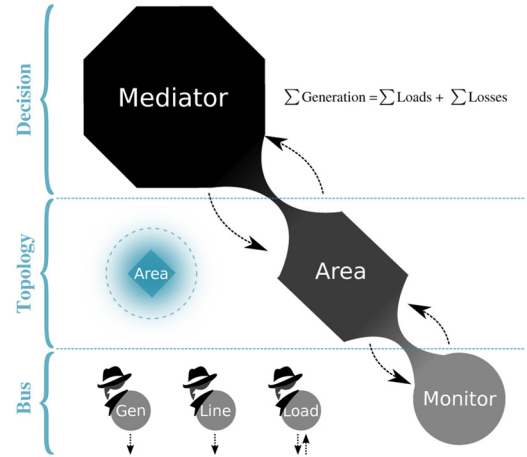


Fig. 1. MAS hierarchical layers.

Each layer is represented by a specific agent type, according to their specific behavior. Eq. (1) illustrates the theoretical necessary amount of agent to implement the proposed MAS.

$$\text{MAS} = \{AG_{\text{Mediator}}, AG_{\text{Area}}^1, \dots, AG_{\text{Area}}^n, AG_{\text{Monitor}}^1, \dots, AG_{\text{Monitor}}^m\} \quad (1)$$

### 2.1. Bus layer

The bus layer is represented by “Monitor Agents”. This type of agent is responsible for taking relevant measurements from the monitored bus. There are three types of Monitor Agents:

- Generation: The power produced by a generator is monitored by “Gen Agents”.
- Line: The power flow through transmission lines is monitored by “Line Agents”. They also check if the line imports or exports power between control areas and if the line is disconnected from the system; and
- Load: The bus power consumption is monitored by “Load Agents”. They are also responsible for receiving the feeder triggering signal, when load shedding is required.

### 2.2. Topology layer

For each control area, there is a single agent associated to the “Topology” layer. This agent holds the information concerning the topology of its area such as: the amount, location and distribution of generators, load buses and interconnected transmission lines. Hence, they are responsible for grouping information from “Monitor Agents” and for making three different equivalent summations: generation, load and transmission values, transferring this information to a higher hierarchical layer agent.

### 2.3. Decision layer

A “Mediator Agent” retains information about the production and consumption of energy resources and has a limited overview of the electrical system. There is only one Mediator Agent in the whole EPS. This type of agent knows how many control areas there are, as well as their overall consumption and generation profile. Moreover, it holds the information about the power flow between the lines that interconnect the control areas. However, this type of agent is not aware of the topology from each control area. Information such as the number of generators, feeders or number of buses and their respective locations are encapsulated by the Monitor Agents. The Mediator Agent takes into account only the power balance between control areas.

The Mediator Agent uses Eq. (2) to make the power balance summation among the control areas of the system. Hence, the active power unbalance and the amount of load to be shed are calculated in each control area. The amount to be shed is transmitted to the Topology Agent to distribute among the “Monitor Load Agents”.

$$\sum \text{Generation} = \sum \text{Loads} + \sum \text{Losses} \quad (2)$$

### 3. Algorithm implementation

For the MAS to be able to work in a coordinated way, the agents are embedded in computational platforms and executed in parallel in real-time platforms. Communication between the various agents is non-blocking, that is, messages received and sent are stored in allocation buffers and processed at run-time. Subscriber type messages are associated with the IEC 61850 protocol for receiving sampled data from the measurement communication channel. GOOSE type messages are exchanged between the measuring device and the MAS by the network infrastructure.

A description of the algorithm concerning the implemented Object-Oriented artifacts is given as follows. In order to describe the behavior of the MAS, a flowchart diagram for each agent type is presented in Fig. 2. The registration procedures send the identification data to the upper layer Agents. An acknowledgement message (Ack) must be returned for each lower layer Agent, confirming that the registration was

successful.

- **Agent Class:** This class defines structures and functions common to all agents, such as the address and communication ports, functions for sending and receiving data and information, data buffers, etc.
- **Monitor Class:** The Monitor class defines objects that perform measurements on the buses that will be installed. Three classes are derived: Generation; Line and Load, each one responsible for monitoring a respective system element. The Load class is also responsible for sending messages to the associated load shedding bus. Fig. 2a illustrates the Monitor Agent behaviour. The white part of the flowchart shows the registration process concerning its respective upper layer (Topology Layer). This step is followed only once. After this step, the Monitor Agent knows the respective Area Agent network address where it should report its measurements. The grey part highlights the agent collected data publishing process, via the IEC 61850 protocol. This is the main loop of this Agent class. In particular, besides the main loop where the collected measured data are published, the specialized Load Monitor Agents need to process the received load shedding messages with the amount of load to be shed and disconnect the appropriate feeders (black part of flow-chart).
- **Area Class:** The Area class holds the information about the topology of a control area. Hence, it aggregates different Monitor type objects, according to the number of generators, interconnection lines and load buses associated with the monitored area. It is also responsible for condensing information, such as generation and consumption and sending it as a single information packet to the upper control layer. Fig. 2b shows the Area Agent behaviour. As well as the Monitor Agent, this type of Agent requests registration for its respective upper layer (Decision Layer), a process shown in white, to be recognized in the system. After this process, the Area Agent knows the network address of the Mediator Agent with whom it should exchange data. All the generation, load and transmission power data from Monitor Agents are shown in gray. These data are aggregated into three separate values (total generation, load and line exchange) and encapsulated in an IEC 61850 message and then sent to the Mediator Agent. This is the main task of the Area Agents. In addition, the Area Agents need to process received load shedding messages from the Mediator Agent and distribute the total amount of load among the load buses. This stage is shown in black in the flowchart.
- **Mediator Class:** This class is responsible for joining general information about the control areas and analyzing fault conditions in the system's elements, islanding events and calculating the need and amount of load shedding. Fig. 2c shows the Mediator Agent behavior. There is no need for registration because the Mediator is a centralized decision Agent, thus there is only one per EPS. All Area Agents must report to this unique entity. The subscribed data messages must contain the summation of three different values of generation, load and power transfer between transmission lines for each topology area. The main function of Mediator Agents is to calculate the energy balance among the system's areas, as well as to send the appropriate load shedding results to the lower layer (Topology Layer). The Mediator decision logic is outlined in Algorithm 1. In the algorithm, the centralized Mediator Agent collects power information about all the power production  $\sum Gen_i$ , power consumption  $\sum Load_i$ , and power transfer between interconnected areas  $\sum Line_i$  for each Area<sub>i</sub> of the EPS. The Mediator Agent then needs to solve Eq. (2) and compute the power unbalance. It is also its responsibility to define if control Area *i* will participate in the (AUFLS) scheme. This is important to differentiate island cases from interconnected system unbalance with several interconnected areas. The unbalance needs to be distributed to the interconnected areas according to a specific criterion. Usually, this action needs to take into consideration the priority classification of each load, considering different aspects,

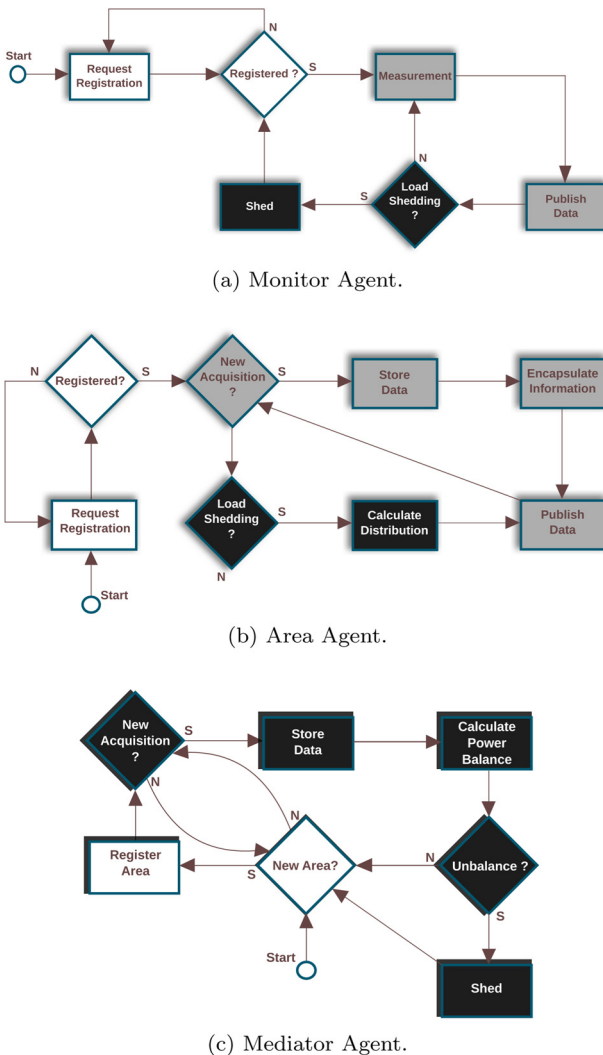


Fig. 2. Agent behavior flowchart.

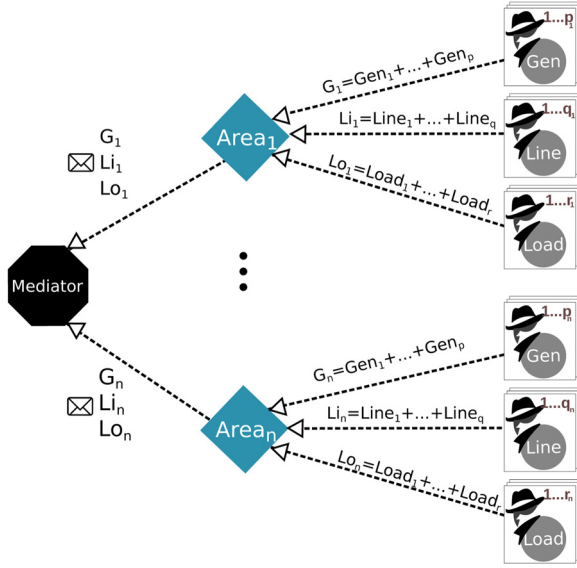


Fig. 3. Data Publishing and Subscribing using GOOSE messages.

such as social, economic, political, impact on the image of the utility company, etc.

#### Algorithm 1. Mediator Agent Decision

```

for all connected Areai do
   $P_{di} = \sum_{i=1}^N \text{Gen}_i + \sum_{i=1}^N \text{Line}_i + \sum_{i=1}^N \text{Load}_i$  {Solve (2)}
  if Areai and  $P_d \leq \epsilon$  then
    select Less Priority Loads (Areai)
    Areai ←  $P_d$ 
  end if
end for

```

Fig. 3 shows the data message exchange between different Agent types. This generic MAS has one Mediator Agent and  $n$  Area Agents. Each Area Agent has its respective amount of Monitor Agents, thus Area 1 has  $p_1$  number of Generation Agents,  $q_1$  Line Agents and  $r_1$  Load Agents. The corresponding index can be deduced for the other Area Agents. An Area Agent condenses all the information about consumption, generation, and transmission into three different values and encapsulates them into a single message. For example, Area<sub>1</sub> sends a message with  $G_1$ ,  $Li_1$  and  $Lo_1$  content. Thus, the upper layer does not have information about the topology of the lower area, such as the number of generation units or the amount of load buses and the feeder location.

Fig. 4 shows the sequence order and exchanging information of the load shedding process. The Mediator Agent calculates the power balance inside each control area, considering the importing and exporting energy flow of transmission lines. Then, if an unbalance is detected, the total amount of power mismatch is sent to the corresponding control

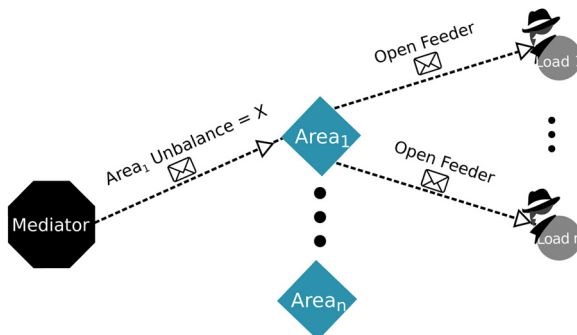


Fig. 4. Load Shedding message exchange.

area. The control area sends the amount of load to be rejected to the respective load buses. In the example of Fig. 4, unintended islanding occurs in Area 1 and the other areas have enough generation to attend their demand, thus the other areas are not affected by the load shedding procedure. The Mediator Agent sends the power mismatch inside its islanding only to Area 1 Agent. The Area 1 Agent calculates the shedding distribution between its load buses and sends the command to disconnect the respective feeders to the appropriate Monitor Load Agents.

#### 3.1. System architecture

A platform consisting of hardware and software was used to reproduce the (AUFLS) solution. The MAS was embedded in this platform and works in real-time for the management and decision-making process of the system. The hardware consists of the RTDS simulator, which allows closed loop configurations, and the embedded computer standard PCI/104 to process the proposed MAS logic. On the other hand, the agents can be installed on any computer platform with real-time and C/C++ code support.

The Real Time Application Interface (RTAI) was chosen because it offers the necessary infrastructure to execute the control and management tasks of the multi-agent solution with Operational System (OS) Linux and C/C++ language support. The IEC 61850 communication protocol is proposed for sampling data transmission among the monitored buses and exchanging information between the upper layer agents. Furthermore, the MAS logic was developed on top of the OpenRelay library code [25,26] and embedded in the PCI/104 hardware platform.

#### 4. Case study

In order to test and validate the proposed methodology, an EPS circuit test was chosen based on the 12-Bus transmission system developed by the IEEE PES Work Group, as a benchmark platform to study the impact of Flexible AC Transmission Systems (FACTS) controllers [27], as shown in Fig. 5. Although the focus of this paper is not directly related to FACTS studies, this benchmark system is adequate to simulate some disturbances related to stability and load shedding, such as: transmission line overloads, power flow variation, inter-area oscillation, over/sub-voltage and over/sub-frequency. To facilitate the HIL requirement, the RTDS platform was selected to model the system in real-time and to provide the closed loop interface via the IEC 61850 protocol.

Three load profiles were considered for the EPS, as shown in Table 1, where  $LB_i$  stands for the active and reactive load at bus  $i$  and  $CB_i$  stands for the capacitor bank at bus  $i$ . The loads were modeled as constant impedances.

As the load profiles were fixed, the intensity of each simulated overload was performed according to several dispatching scenarios. Table 2 shows the variation in active power adopted for each generator. A spinning reserve of 10% in each case was considered.

The stability study parameters are shown in Table 3. The EPS has a 60 Hz nominal frequency and small variations within the  $\pm 0.5$  Hz range are permissible. The presence of steam turbines limits the maximum and minimum frequency to 63.0 Hz and 56.5 Hz, respectively, before the generators' protection is triggered. In order to prevent improper operation of (AUFLS) schemes and allow the spinning reserve to be used in overload cases of small magnitude, a supervisory frequency threshold of 58.5 Hz was established. A stability study analysis was performed in order to obtain the potential contingency events that could lead to an under frequency condition. In this phase, for the analysed power system case study, the potential events for each control area are listed in Table 3. The load profile was weighted according to the relative probability of occurrence.

Fig. 6 shows the network infrastructure built in order to execute the



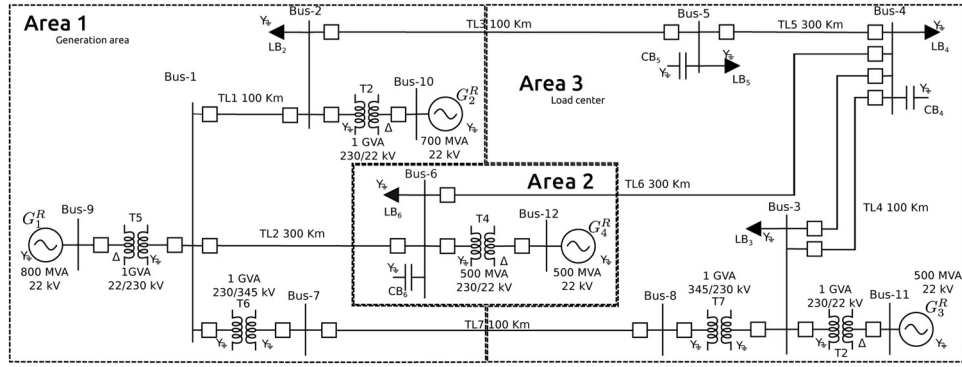


Fig. 5. Electrical power system simulated.

**Table 1**  
Loads connected to the power system.

		Light load		Medium load		Heavy load	
		MW	MVar	MW	MVar	MW	MVar
Area 1	LB <sub>2</sub>	253.3	107.9	316.6	134.9	364.1	155.1
	LB <sub>6</sub>	392.0	167.0	489.9	208.7	563.4	240.0
Area 3	CB <sub>6</sub>	–	180.0	–	180.0	–	180.0
	LB <sub>3</sub>	294.4	125.4	368.0	156.8	423.2	180.3
	LB <sub>4</sub>	294.4	125.4	368.0	156.8	423.2	180.3
	LB <sub>5</sub>	85.83	36.6	107.3	45.7	123.4	52.6
	CB <sub>4</sub>	–	160.0	–	160.0	–	160.0
	CB <sub>5</sub>	–	80.0	–	80.0	–	80.0

**Table 2**  
Configuration of generation units.

Gen	Capacity (MVA)	Reserve (%)	Light	Load (MW)	Medium	Heavy
$G_1^R$	800	10	[150–450]	[180–580]	[190–690]	
$G_2^R$	700	10	[100–400]	[100–500]	[100–600]	
$G_3^R$	500	10	[270–500]	[360–500]	[370–500]	
$G_4^R$	500	10	[280–400]	[350–500]	[400–500]	

**Table 3**  
General description of the EPS stability study parameters.

Parameter	Description
Frequency	Limits
	$f_{max}$ : 63 Hz $f_{min}$ : 56.5 Hz
Stability	$f_{smax}$ : 60 + 0.5 Hz $f_{smin}$ : 60 – 0.5 Hz
Supervision	$f_{sup}$ : 58.5 Hz
Maximum overload	Area 1: 30%
	Area 2: 30%
	Area 3: 60%
Contingency	Area 1: Loss of G2
	Area 2: Area 2 Islanding (TL <sub>2</sub> and TL <sub>6</sub> )
	Area 3: Area 3 Islanding (TL <sub>3</sub> , TL <sub>6</sub> and TL <sub>7</sub> )
Load Profile	<b>Profile Percentage</b>
	Light: 70%
	Medium: 85%
	Heavy: 100%
Relative probability	0.3
	0.5
	0.2

HIL apparatus. The amount of installed Agents can be defined using the parameters of Eq. (1). Only one central Mediator Agent was installed. As the system has three control areas,  $n = 3$  was defined. Furthermore, the system has 4 generation units, 5 load buses and 3 inter-area transmission lines. Therefore,  $m = 12$  was assumed. All the Agents were installed in the same processing unit, showing that if a communication link to the measured data is available, such as the use of the IEC 61850 protocol, there is no need to install Agents physically in

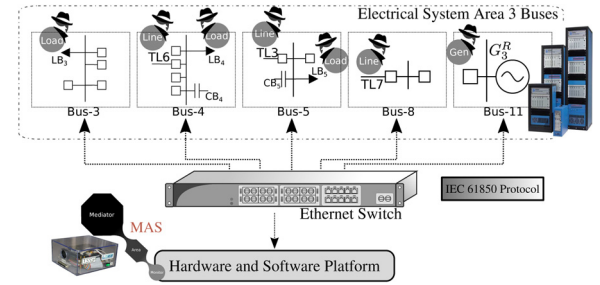


Fig. 6. Network infrastructure.

different buses, reducing the cost of the proposed solution.

For the sake of clarity, only Area 3 monitored buses and the allocated agents are represented. The EPS is simulated in real-time via RTDS hardware. The RTDS platform provides the required IEC 61850 interfaces to exchange information about the monitored bus output signals and the input commands to shed the appropriate loads. The closed loop is performed through the Ethernet switch with IEC 61850 capabilities. In real scenarios, the monitored buses are distributed into several substations (in a specific control area) and several computational platforms would be necessary to execute the MAS solution. For the simulated system, all the buses are available locally and, therefore, only one piece of PCI/104 hardware was used to run all the agents involved.

Although the 12-Bus EPS is used as a test system to validate the multi-agent proposal, it is important to note that the methodology was structured generically and can be applied to any network topology structured in control areas.

## 5. Performance evaluation

The (AUFLS) design for the 12-Bus EPS was based on the parameters described in Table 3. The amount of load to be shed is calculated in real time from the MAS logic operation. Two different scenarios were chosen to illustrate the MAS behavior. The ideal load shedding amount, considering no changes to the system's state, is the unbalance result of Eq. 2 before the application of any contingency. Thus, if the contingency scenario is the loss of generation, then the ideal load shedding amount will be the power provided by the corresponding generation. If the contingency scenario is an intentional islanding, then the ideal load shedding amount is the difference between the whole available generation capacity and the total load demand inside the islanding area, before the contingency occurrence.

Fig. 7a shows an example of Area 2 islanding. Transmission lines  $T_2$  and  $T_6$  interconnect Area 2 with the rest of the system. When a fault occurs in  $T_2$  and the automatic protection system is activated, all the power flows through  $T_6$ , surpassing the maximum power transmission capacity of this line, generating a voltage instability problem. In order

to mitigate this event and avoid affecting the whole infrastructure of Area 2,  $T_6$  is also disconnected from the system creating an isolated area. Even considering this islanding configuration, the proposed MAS is capable of executing the load shedding algorithm and maintaining the stability of the system because only the electrical part of the system was disconnected, not the data transmission capability. With 400 MW of generation in  $G_4$  in a medium load profile, Area 2 frequency starts to decrease, as 400 MW is not enough to provide power to the internal load. After the frequency is below the supervisory value (58.5 Hz), the MAS acts, removing 95.53 MW of the total load (19%) of Area 2, restoring the frequency close to the nominal value without affecting any load of the remaining areas.

Fig. 7a also shows that Area 1 and Area 3 do not experience an underfrequency scenario. Instead there is a rebound effect, increasing the frequency of these two areas because of the disconnection of the full load block of Area 2. It can be observed that the amount of disconnected loads are almost the same as the ideal one.

In a second scenario, Fig. 7b represents a generation loss contingency.  $G_1$  (500 MW) operating in a heavy load profile is disconnected, affecting the frequency of the overall system. All control areas are affected by its disconnection and the frequency decreases below the supervisory value (58.5 Hz). The MAS distributes the load shedding between the areas, removing 109.23, 169.02 and 290.94 MW from Area 1, Area 2 and Area 3, respectively, totalizing 569.19 MW of disconnected load. This corresponds to a 30% of load disconnection in each area (equally distributed), i.e., the same power unbalance on the entire connected system. The sum of all disconnected load blocks is similar to the ideal load shedding amount.

According to [28], the maximum time latency for synchrophasor-based real-time state estimation application is 100 ms, including latencies for PMU signal acquisition, PMU synchrophasor estimation and data encapsulation, communication network delay, PDC data frame time alignment, bad data detection, and state estimation. The dynamics of large power systems do not allow fast changes in their frequency due to the kinetic energy of the generator's rotational inertia. Therefore, the frequency decay is not an abrupt event. The load shedding process needs to allow a frequency decay below a specified value (58.5 Hz in the power system analysed) in order to take any corrective action. The process to stabilise the frequency can happen in a time range of a few seconds before any automatic protection element is activated. Having good load shedding algorithms that can calculate the necessary load shed amount in a few steps, such as the proposed method, does not require restricted time delay limits.

The results represented in Fig. 7 show a good performance of the multi-agent system. The two different scenarios (islanding of one of the areas and generation loss of a connected system) have been processed with good accuracy and very close to the ideal shedding amount. The accuracy of the multi-agent system will be better explained in Fig. 10. Although the shedding algorithm is designed to adapt to the unbalance between generation and demand in real time, only one step was sufficient to establish the balance and the control over the frequency decay in all simulated cases within a feasible time delay.

### 5.1. Comparison with other methods

In order to evaluate the MAS performance, the results were compared with two other load shedding philosophies: the instantaneous frequency of the system ( $f$ ) and the (ROCOF) ( $\frac{df}{dt}$ ). In order to do that, a scoring metric system capable of synthesizing (in only one absolute value) the performance of each individual scheme is very useful. There is a lack of studies in the literature concerning the comparison among different AUFLS philosophies.

The performance comparison is based on a previous paper published by the authors in [23]. In this paper, a generic score metric system is proposed that can be applied to different load shedding schemes

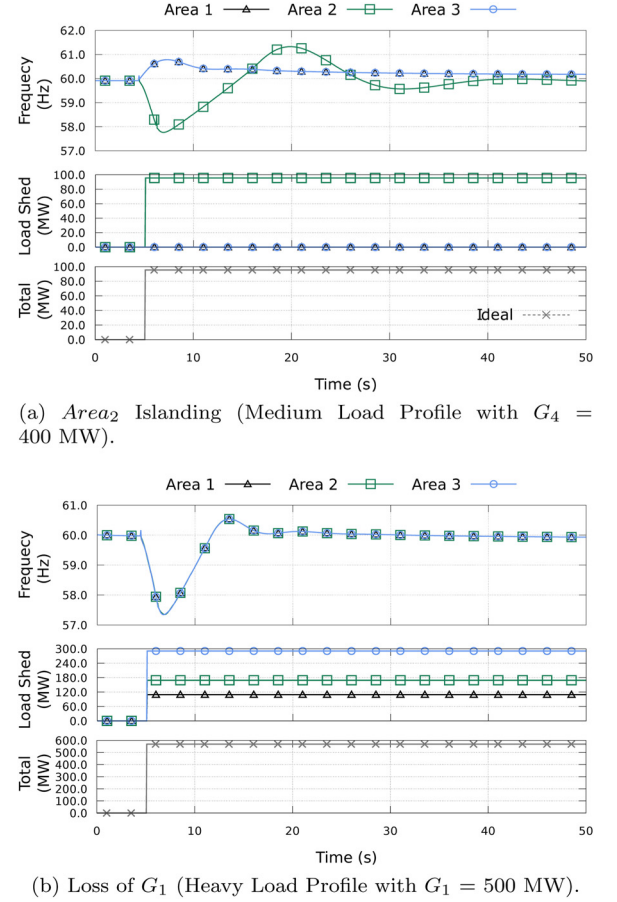


Fig. 7. Load shedding cases.

regardless of the power system being analysed. The metric considers several schemes and evaluates different load shedding parameters and set points in order to select the winner candidate. The metric score system was applied to the same case study in both papers, using the same methodology. The comparison indicates that the multi-agent solution can score better than traditional load shedding schemes.

For additional information regarding the frequency behavior and the impact of each AUFLS scheme, the frequency curves of each overload case were considered. Equation (3) shows the metric composition of a scheme ( $i$ ) with a generic load profile ( $L$ ). Each scheme ( $i$ ) is formed by a domain with several frequency curves ( $j$ ), representing each simulated overload case. The best scheme is the one with the lowest score. The metric comprises three terms and each one is responsible for evaluating the performance of a shedding scheme in a different perspective related to the stability concept:

- The area comprising the maximum and minimum frequency during frequency oscillation;
- The penalty magnitude sum of the values that exceed the allowed thresholds; and
- The average time that the system frequency returns to a given range of tolerance around its nominal value (settling time).

$$\text{Score}_i^L = \text{Area}_i^L + \sum_{j \in i} \text{Mag}_j^L(j) + \text{mean}_{j \in i} \{T_s^L(j)\} \quad (3)$$

A detailed study was performed by the authors, considering the same EPS of Section 4. Table 4 shows the load shedding logic for the three areas using both philosophies. This procedure was followed in order to find the final configuration parameters, such as the number of steps, the frequency and derivative thresholds and the distribution of

**Table 4**  
Conventional load shedding schemes.

		Area 1		Area 2		Area 3	
Instant. frequency	step	Freq (Hz)	Shed (%)	Freq (Hz)	Shed (%)	Freq (Hz)	Shed (%)
	1	58.50	20	58.50	10	58.50	30
	2	57.50	10	58.10	8	57.83	20
	3	–	–	57.70	6	57.17	10
	4	–	–	57.30	4	–	–
	5	–	–	56.90	2	–	–
ROCOF	step	Freq (Hz/s)	Shed (%)	Freq (Hz/s)	Shed (%)	Freq (Hz/s)	Shed (%)
	1	–0.1	5	–0.1	6	–0.1	4
	2	–0.8	10	–0.5	6	–0.5	8
	3	–1.4	15	–0.9	6	–0.9	12
	4	–	–	–1.3	6	–1.3	16
	5	–	–	–1.7	6	–1.7	20

load among steps for each methodology. The aim is to compare the performance of the new proposed method with those obtained from the other shedding philosophies.

It should be mentioned that 9620 cases were simulated, divided into three load profiles, three load distributions, six possible steps, three contingencies considering the three control areas and sixty variations of generation in steps of 2 MW, each one taking 70s of execution time, totaling 189h of simulation.

In order to illustrate the performance of each philosophy, a shedding case is presented in Fig. 8. This case corresponds to an islanding occurrence in Area 2, having 400 MW of generation in  $G_4$ . The figure shows the frequency curve before, during and after the contingency. On the subsequent curves the trigger time for each philosophy is presented and compared with the ideal value.

In the first section of Fig. 8, the frequency curves show that the MAS presented the least disturbance of the system frequency. This occurs because the amount of load shed was the closest to the ideal value (18%). The removal of larger load blocks tends to increase the over-frequency rebound effect. The other two philosophies must adapt the amount of load shed, according to the number of steps available, therefore, a larger variation is presented.

The MAS and the (ROCOF) philosophies presented the same trigger time (0.4 s). This occurs because these schemes calculate the energy deficit at the beginning of the contingency. When the system frequency reaches the supervisory frequency (58.5 Hz), the shedding trip command is sent by the appropriate load buses. On the other hand, the instantaneous frequency method waits for the frequency decay in each configured frequency levels, and, therefore needs three shedding steps to achieve the system stability that corresponds to a 3.5 s delay response. The shedding accuracy of each philosophy is presented in

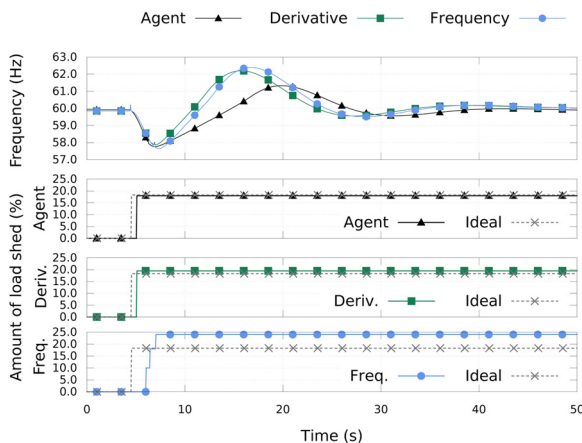


**Fig. 8.** Load shedding case: Area 2 islanding with  $G_4 = 400$  MW.

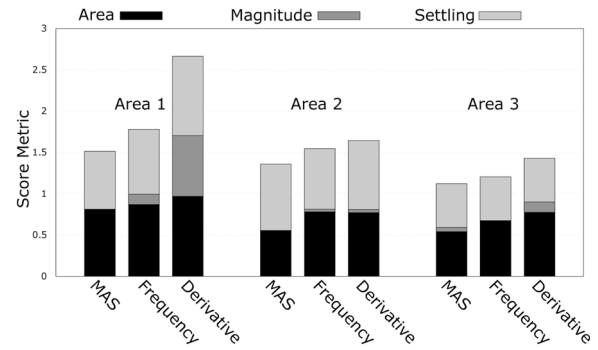


**Fig. 9.** Score metric for each control area.

**Fig. 10.**

Fig. 9 shows the final scoring metric evaluation of each methodology, concerning the area, magnitude and average settling time of all tested cases. The metric evaluation gives a normalized average score within the range [0, 1] for each category. The MAS solution presented better scoring in all control areas with great emphasis on the magnitude values that are close to zero, demonstrating that this philosophy had few cases that exceeded the generator protection thresholds. On the other hand, the derivative philosophy had the worst results, specially for Area 1 that achieved a total score of 2.7 and high magnitude component. This philosophy usually sheds large load blocks at the beginning of the shedding process, therefore, causing greater disturbance to the system frequency. The instantaneous frequency method presented an intermediate alternative.

## 5.2. Comparison of the Load Shedding Errors

The effectiveness of each shedding philosophy is evaluated by analyzing the amount of load shed in each overload situation. A good shedding philosophy must shed an amount of load as close as possible to the ideal value, i.e., the amount of load which brings the system to the balanced state. The unnecessary load disconnection causes financial losses and negative consequences to residential, commercial and industrial customers. On the other hand, the insufficient shedding could be incapable of establishing the frequency balance, affecting the equipment and the EPS integrity, especially the generators.

In order to show the load shedding error distribution and avoid generalization of only one measure, such as the mean error, the statistic tool called *boxplot* was chosen to represent the error concerning the load shedding data. In a single diagram, the boxplot can represent all the samples ordered by magnitude and the following parameters: minimum value, first quartile, median (second quartile), third quartile and maximum value. The first quartile, or lower quartile, delimits 25% of the samples. The median, or second quartile, defines the cutoff range, representing 50% of the total samples, while the third quartile, or upper quartile, delimits 75% of the samples. Thus, the "box" represented by the quartiles concentrate 50% of the total distribution. The whiskers extend from each end of the box for a range equal to 1.5 times the interquartile range (i.e. the vertical height of the box). Each whisker is truncated back toward the median so that it terminates at a y value belonging to some point in the error data set. Since there may be no point whose value is exactly 1.5 times the interquartile distance, the whisker may be shorter than its nominal range. Any points that lie outside the range of the whiskers are considered outliers and are represented by isolated points outside the boxplot representation.

The absolute error of all tested cases for each control area are shown in Figs. 10a, b and c, respectively. The MAS solution obtained the lowest median of shedding errors when compared with the other two philosophies for all control areas and all load profiles. The biggest error registered for the MAS solution was about 10%, when considering control area 2 with a heavy load profile. As for the instantaneous

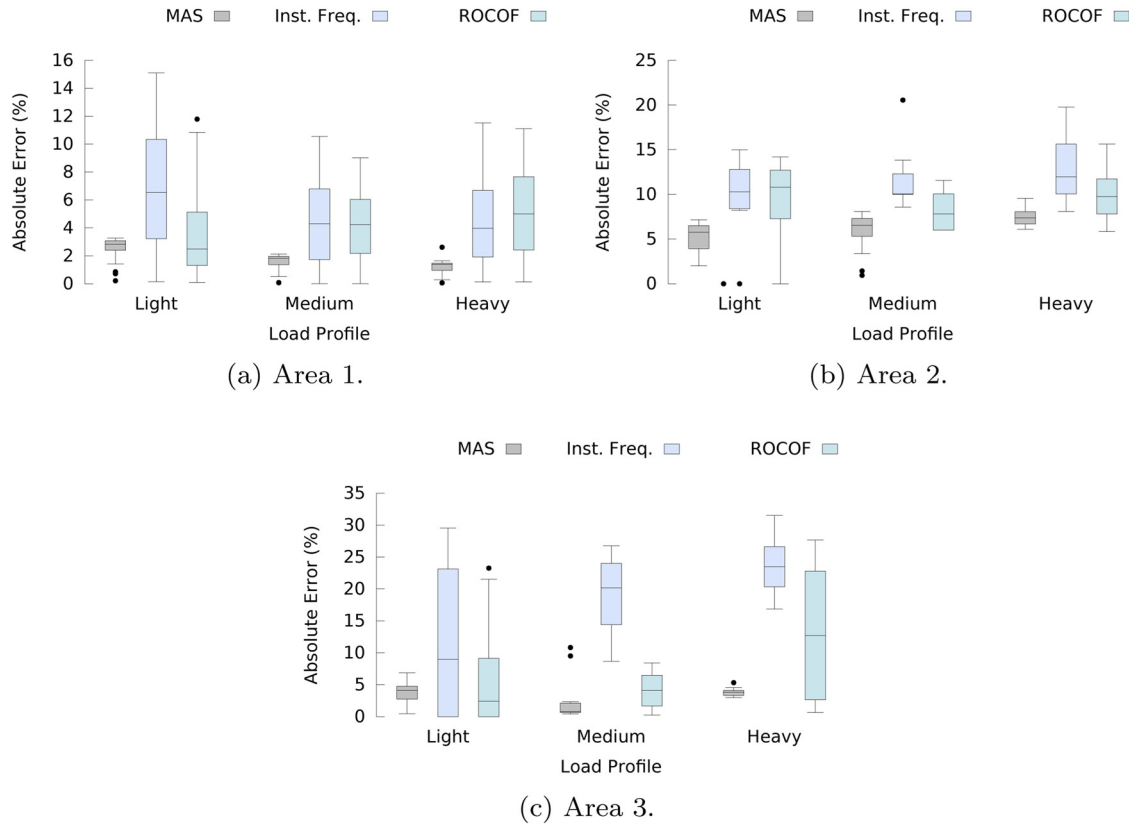


Fig. 10. Absolute error of the amount of load shed.

frequency and (ROCOF) philosophies, the biggest errors obtained were about 35% and 30%, respectively, when considering control area 3 with a heavy load profile.

The extent of the *boxplot* also presented different characteristics. The quartiles show that the MAS errors were concentrated very close to the median, as well as the maximum and minimum values. The majority of the outliers were concentrated in values below the minimum error, showing the effectiveness of the load shedding algorithm. On the other hand, the instantaneous frequency and (ROCOF) philosophies showed more extensive bodies and the maximum values reached higher magnitudes, showing that errors may differ drastically from the median. Moreover, the score value obtained by the instantaneous frequency method is achieved at the cost of an excessive shed. Therefore, the MAS solution is considered the best scheme for the (AUFLS) design, presenting the best scoring values and obtaining the lowest error distribution.

## 6. Conclusion

This paper proposes a new centralized MAS that coordinates the various stages of (AUFLS) processes. The new philosophy presented a scalable architecture regardless of the EPS analysed, representing a relevant contribution to the stability and protection of the system. The load shedding was performed seeking the minimum impact on the system in the shortest period of time.

The results demonstrate the feasibility of the proposed methodology. The MAS proved to be a good alternative compared to conventional philosophies. The shedding was carried out in a single step, providing a fast and effective restoration of the system's frequency. Moreover, the absolute error associated with the amount of load effectively shed and the ideal amount was substantially better if compared with the other two methodologies implemented.

Although the results showed that only one step was enough to

prevent the frequency decay in different scenarios, it is worth mentioning that the proposed method is an iterative solution. The proposed algorithm has a general approach regarding any load bus of the system. The Monitor Agent indicates only the necessary percentage of load removal concerning the specified monitored bus. Considering this, it is possible for each application to define their own priority levels and configure them to the appropriate feeders without any changes in the proposed method.

The real-time development platform consisting of PCI/104 hardware with the real-time software RTAI and the OpenRelay library showed to be a good alternative to the design of the MAS architecture. Using the RTAI not only facilitated the resource management, especially providing communication interfaces using the IEC 61850 protocol, but also allowed for the expansion of the OpenRelay library using C/C++ code.

The MAS applied to the 12-Bus EPS has complied with the real-time requirements of the circuit simulation via RTDS. The topology of the electrical system, as well as its characteristics and dynamic parameters were considered so that the operating times and expected results were close to the situations encountered in actual environments. The MAS improved the decision-making in the (AUFLS) field and, consequently, contributed to maintaining the system's stability and prevention of blackouts.

No consideration was made regarding signal noise, imprecision on digital system conversion and their impact on the system behavior. Given the importance of such effects, a detailed investigation of these issues will be made in the future concerning how they can influence the final behavior of our methodology and the response of traditional (AUFLS), such as the calculation of the (ROCOF) values and, ultimately the performance of the MAS.

Our future research should also be directed towards high energy production in distributed generation environments. In order to accommodate this new reality, some modifications need to be



implemented. However, the authors believe in the feasibility of such a scenario, using the same methodology adopted in this paper. Most of the changes will concentrate only on the Monitor Agent.

## Acknowledgement

The authors would like to acknowledge the University of São Paulo (Brazil) and the Center for Energy Informatics, Mærsk Mc-Kinney Møller Institutet, University of Southern Denmark for the research facilities provided to conduct this project. This study was financed in part by the Coordenação de Aperfeiçoamento de Pessoal de Nível Superior – Brasil (CAPES) – Finance Code 001. Our thanks also extend to the financial support received from FAPESP Fundação de Amparo à Pesquisa do Estado de São Paulo grant #2017/16742-7.

## References

- [1] J. Guo, F. Liu, S. Huang, L. Chen, W. Wei, L. Ding, Towards optimal estimation of blackout probability based on sequential importance sampling simulations, 2017 IEEE Power Energy Society General Meeting (2017) 1–5, <https://doi.org/10.1109/PESGM.2017.8274059>.
- [2] P. Hines, J. Apt, S. Talukdar, Large blackouts in North America: Historical trends and policy implications, *Energy Policy* 37 (12) (2009) 5249–5259, <https://doi.org/10.1016/j.enpol.2009.07.049>.
- [3] U. Rudez, R. Mihalic, Monitoring the first frequency derivative to improve adaptive underfrequency load-shedding schemes, *IEEE Trans. Power Syst.* 26 (2) (2011) 839–846, <https://doi.org/10.1109/TPWRS.2010.2059715>.
- [4] Gierisch, W.C., Load reduction by underfrequency relays during system emergencies [includes discussion], *Power Apparatus and Systems, Part III. Transactions of the American Institute of Electrical Engineers*, 73, 2, 10.1109/AIEEPAS.1954.4499015.
- [5] P. Anderson, M. Mirheydar, An adaptive method for setting underfrequency load shedding relays, *IEEE Trans. Power Syst.* 7 (2) (1992) 647–655, <https://doi.org/10.1109/59.141770>.
- [6] V. Chuvychin, N. Gurov, S. Venkata, R. Brown, An adaptive approach to load shedding and spinning reserve control during underfrequency conditions, *IEEE Trans. Power Syst.* 11 (4) (1996) 1805–1810, <https://doi.org/10.1109/59.544646>.
- [7] P. Zhang, F. Li, N. Bhatt, Next-generation monitoring, analysis, and control for the future smart control center, *IEEE Trans. Smart Grid* 1 (2) (2010) 186–192, <https://doi.org/10.1109/TSG.2010.2053855>.
- [8] S. Padrón, M. Hernández, A. Falcón, Reducing under-frequency load shedding in isolated power systems using neural networks. gran canaria: A case study, *IEEE Trans. Power Syst.* 31 (1) (2016) 63–71, <https://doi.org/10.1109/TPWRS.2015.2395142>.
- [9] J. Jallad, S. Mekhilef, H. Mokhlis, J.A. Laghari, Improved ufls with consideration of power deficit during shedding process and flexible load selection, *IET Renew. Power Gen.* 12 (5) (2018) 565–575, <https://doi.org/10.1049/iet-rpg.2017.0170>.
- [10] W. Liu, W. Gu, W. Sheng, X. Meng, Z. Wu, W. Chen, Decentralized multi-agent system-based cooperative frequency control for autonomous microgrids with communication constraints, *IEEE Trans. Sustain. Energy* 5 (2) (2014) 446–456, <https://doi.org/10.1109/TSTE.2013.2293148>.
- [11] F. Augusto de Souza, C. Unsihuay Vila, F. Enembreck, L. Martins Carpes, A multi-agent framework for self-healing mechanisms considering priority-based load shedding and islanding with distributed generation in smart distribution grids, *IEEE Latin America Transactions* 15 (4) (2017) 632–638, <https://doi.org/10.1109/TLA.2017.7896348>.
- [12] R. Hooshmand, M. Moazzami, Optimal design of adaptive under frequency load shedding using artificial neural networks in isolated power system, *Int. J. Electr. Power Energy Syst.* 42 (1) (2012) 220–228, <https://doi.org/10.1016/j.ijepes.04.2012.021>.
- [13] H. Mortaji, S.H. Ow, M. Moghavvemi, H.A.F. Almurib, Load shedding and smart-direct load control using internet of things in smart grid demand response management, *IEEE Trans. Ind. Appl.* 53 (6) (2017) 5155–5163, <https://doi.org/10.1109/TIA.2017.2740832>.
- [14] X. Xie, D. Yue, C. Peng, Relaxed real-time scheduling stabilization of discrete-time takagi-sugeno fuzzy systems via an alterable-weights-based ranking switching mechanism, *IEEE Trans. Fuzzy Syst.* 26 (6) (2018) 3808–3819, <https://doi.org/10.1109/TFUZZ.2018.2849701>.
- [15] J.A. Laghari, H. Mokhlis, M. Karimi, A.H.A. Bakar, H. Mohamad, A new under-frequency load shedding technique based on combination of fixed and random priority of loads for smart grid applications, *IEEE Trans. Power Syst.* 30 (5) (2015) 2507–2515, <https://doi.org/10.1109/TPWRS.2014.2360520>.
- [16] M.G. Darebaghi, T. Amraee, Dynamic multi-stage under frequency load shedding considering uncertainty of generation loss, *IET Gen. Transmission Distrib.* 11 (13) (2017) 3202–3209, <https://doi.org/10.1049/iet-gtd.2016.0751>.
- [17] U. Rudez, R. Mihalic, Wams-based underfrequency load shedding with short-term frequency prediction, *IEEE Trans. Power Del.* 31 (4) (2016) 1912–1920, <https://doi.org/10.1109/TPWRD.2015.2503734>.
- [18] J.D.L. Ree, V. Centeno, J.S. Thorp, A.G. Phadke, Synchronized phasor measurement applications in power systems, *IEEE Trans. Smart Grid* 1 (1) (2010) 20–27, <https://doi.org/10.1109/TSG.2010.2044815>.
- [19] A. Chakraborty, J.H. Chow, A. Salazar, A measurement-based framework for dynamic equivalencing of large power systems using wide-area phasor measurements, *IEEE Trans. Smart Grid* 2 (1) (2011) 68–81, <https://doi.org/10.1109/TSG.2010.2093586>.
- [20] D. Ghosh, T. Ghose, D.K. Mohanta, Communication feasibility analysis for smart grid with phasor measurement units, *IEEE Trans. Ind. Inform.* 9 (3) (2013) 1486–1496, <https://doi.org/10.1109/THI.2013.2248371>.
- [21] F. Li, W. Qiao, H. Sun, H. Wan, J. Wang, Y. Xia, Z. Xu, P. Zhang, Smart transmission grid: Vision and framework, *IEEE Transactions on Smart Grid* 1 (2) (2010) 168–177, <https://doi.org/10.1109/TSG.2010.2053726>.
- [22] Y. Yan, Y. Qian, H. Sharif, D. Tipper, A survey on smart grid communication infrastructures: Motivations, requirements and challenges, *IEEE Communications Surveys Tutorials* 15 (1) (2013) 5–20, <https://doi.org/10.1109/SURV.2012.021312.00034>.
- [23] A.Q. Santos, R.M. Monaro, D.V. Coury, M. Oleskovicz, New scoring metric for load shedding in multi-control area systems, *IET Generation, Transmission & Distribution* 11 (5) (2017) 1179–1186.
- [24] IEEE Std C37.117, IEEE guide for the application of protective relays used for abnormal frequency load shedding and restoration, *IEEE Std C37.117-2007* (2007) 1–55, <https://doi.org/10.1109/IEEESTD.2007.4299516>.
- [25] R.M. Monaro, Openrelay Available in: <https://github.com/renato-monaro/OpenRelay>. February 23, 2016. (October 2015).
- [26] R.M. Monaro, A.Q. Santos, S. Santo, D. Coury, A. Aguiar, Openrelay: Open source protection algorithms for electric power system relays, *IEEE Power Engineering Society General Meeting* (2018).
- [27] S. Jiang, U.D. Annakkage, A.M. Gole, A platform for validation of facts models, *IEEE Trans. Power Del.* 21 (1) (2006) 484–491, <https://doi.org/10.1109/TPWRD.2005.852301>.
- [28] B. Yang, K.V. Katsaros, W.K. Chai, G. Pavlou, Cost-efficient low latency communication infrastructure for synchrophasor applications in smart grids, *IEEE Syst. J.* 12 (1) (2018) 948–958, <https://doi.org/10.1109/JSYST.2016.2556420>.